

# Effect of ammonium polyacrylate on rheology of anatase TiO<sub>2</sub> nanoparticles dispersed in silicon alkoxide sols

Wenjea J. Tseng\*, Jolin Nian

*Department of Materials Engineering, National Chung Hsing University, 250 Kuo Kuang Road, Taichung 402, Taiwan, ROC*

Received 17 September 2003; received in revised form 12 December 2003; accepted 12 January 2004

Available online 21 April 2004

## Abstract

Ammonium polyacrylate (NH<sub>4</sub>PA) was introduced into powdered mixtures consisting of anatase-structured TiO<sub>2</sub> nanoparticles and silicon alkoxide precursors at the sol level, and the rheological behavior of the mixtures was examined under various solid loadings ( $\phi = 0.05$ – $0.13$  in volumetric ratios), shear rates ( $\dot{\gamma} = 1$ – $1000 \text{ s}^{-1}$ ) and NH<sub>4</sub>PA concentrations. The alkoxide precursors were mixtures of tetraethyl orthosilicate (TEOS, Si(OC<sub>2</sub>H<sub>5</sub>)<sub>4</sub>), ethyl alcohol (C<sub>2</sub>H<sub>5</sub>OH), H<sub>2</sub>O and HCl in a constant [H<sub>2</sub>O]/[TEOS] ratio of 11. The nanoparticle–sol mixtures generally exhibited a pseudoplastic flow behavior over the shear-rate regime examined. The NH<sub>4</sub>PA appeared to serve as an effective surfactant which facilitates the suspension flow by reducing the flow resistance at low NH<sub>4</sub>PA concentrations. At  $\phi = 0.10$ , a viscosity reduction ca. 85% was found at  $\dot{\gamma} = 10 \text{ s}^{-1}$  when the NH<sub>4</sub>PA concentration was held at 2.5 wt.% of the solids. As the NH<sub>4</sub>PA exceeded a critical level, e.g., [NH<sub>4</sub>PA]  $\geq 3.0$  wt.%, the NH<sub>4</sub>PA acted as a catalyst which quickly turned the TiO<sub>2</sub>–silica sol mixtures ( $\phi = 0.10$ ) into a gelled structure, resulted in a pronounced increase of mixture viscosity. The maximum solids concentration ( $\phi_m$ ) of the mixtures was experimentally determined from a derivative of relative viscosity, i.e.,  $(1 - \eta_r^{-1/2})$ – $\phi$  dependence. The estimated  $\phi_m$  increased from 0.127 to 0.165 when NH<sub>4</sub>PA of 0.5 wt.% was introduced into the TiO<sub>2</sub>–silica sol mixtures.

© 2004 Elsevier Ltd and Techna S.r.l. All rights reserved.

**Keywords:** D. TiO<sub>2</sub>; Sol–gel; Surfactant; Rheology; Aggregation

## 1. Introduction

TiO<sub>2</sub>–SiO<sub>2</sub> composites in thin film or colloidal form are materials of great technological interests. The interests mainly stem from the generation of highly potent oxidants (i.e., holes) at the semiconductor surface when the wide-bandgap semiconducting material (i.e., TiO<sub>2</sub>) is illuminated by light. The oxidant generation allows for the use of the composite materials in photocatalytic detoxification process of aquatic environments. An enhanced photocatalytic performance of particulate TiO<sub>2</sub>–SiO<sub>2</sub> mixtures has been reported [1–4], which surpassed the photodecomposition efficacy of pure, anatase TiO<sub>2</sub> phase. The existence of SiO<sub>2</sub> is thought to change the surface acidity of the composites [2], producing effective adsorption sites of significantly larger population than that of the pure TiO<sub>2</sub>. These sites are desirable at locations near the photocatalytic TiO<sub>2</sub> phase in order to facilitate a rapid scavenging of holes

generated from the oxidants (e.g., hydroxyl radicals). Recombination of the photogenerated electron (e<sup>−</sup>) and hole (h<sup>+</sup>) is then suppressed, leading to an increased quantum yield.

Various methods have been used to fabricate the TiO<sub>2</sub>–SiO<sub>2</sub> composites. These include sol–gel solution technique, impregnation, homogeneous precipitation, flame pyrolysis and ion-beam implantation [5,6]. With the sol–gel technique, in particular, the chemical composition can be well controlled in molecular-level mixing, and a composite structure with a high specific surface area together with a well-defined pore-size distribution ranging in mesoporous region is attainable. In addition, the isolated Ti–O–Si centers are resistant to leaching so that this type of catalyst can be used as a highly active and selective catalyst for partial oxidation of liquid-phase hydrocarbons under very mild operating conditions [6]. When TiO<sub>2</sub> and SiO<sub>2</sub> powders were used as the starting material for the composite mixtures, Richmond et al. [7] pointed out that the TiO<sub>2</sub> particles adsorb preferentially on the SiO<sub>2</sub> particle surfaces, forming SiO<sub>2</sub> aggregates with the TiO<sub>2</sub> particles coated on the surface. This changed the

\* Corresponding author. Fax: +886-4-2285-7017.

E-mail address: wenjea@dragon.nchu.edu.tw (W.J. Tseng).

surface characteristics of the particles, as well as the structure of the composite mixtures and the mixture rheology. In this regard, we present here a method to fabricate uniform  $\text{TiO}_2$ – $\text{SiO}_2$  composites through mixing of anatase-structured  $\text{TiO}_2$  nanoparticles with silicon alkoxide precursors to form “flowable” powdered dispersions. A uniform dispersion of  $\text{TiO}_2$  nanoparticles in the silica sol with a high Ti/Si ratio is aimed so that the powdered dispersion may later be “consolidated” into a gelled structure with desirable function and hierarchy via typical wet-processing routes. A surfactant of ammonium polyacrylate ( $\text{NH}_4\text{PA}$ ) is introduced into the nanoparticle mixtures, and the effect of the  $\text{NH}_4\text{PA}$  to the dispersion quality of the mixtures is examined via rheological characterizations.

## 2. Experimental procedure

$\text{TiO}_2$  nanoparticles (P25, Degussa Ltd., Germany) with an average particle size about 21 nm and a specific surface area  $50 \pm 15 \text{ m}^2/\text{g}$  (vendor specification) were used as the starting material. The powder is about rectangle in shape and is apparently agglomerated (Fig. 1) from the scanning electron microscopy (SEM, JSM6700F, JEOL, Japan). Reagent-grade tetraethyl orthosilicate (TEOS,  $\text{Si}(\text{OC}_2\text{H}_5)_4$ ), ethyl alcohol ( $\text{C}_2\text{H}_5\text{OH}$ ),  $\text{H}_2\text{O}$  and  $\text{HCl}$  (all from Aldrich Chemicals) in a constant  $[\text{H}_2\text{O}]/[\text{TEOS}]$  ratio of 11 were used as the precursor sol and were mixed

with the nanoparticles in various volumetric solids concentrations ( $\phi = 0.05$ – $0.13$ ). The polyelectrolyte surfactant used was a commercially available ammonium polyacrylate ( $\text{NH}_4\text{PA}$ , A-6114, Toagosei Chemical, Japan) and the surfactant concentration was up to 3 wt.% of the solids. The  $\text{NH}_4\text{PA}$  typically presents a linear backbone consisting of carbon–carbon bonds, with a  $\text{COONH}_4$  side group attached to the carbon atom [8].

The powdered mixtures were ball-mixed in polyethylene bottles using high-purity alumina balls as the mixing media for 24 h. Their viscosity ( $\eta_s$ ) was determined by a strain-controlled concentric viscometer (VT550, Gebrüder HAAKE GmbH, Germany) equipped with a sensor system (MV-DIN 53019, HAAKE, Germany) of a cone-cup geometry operated at a constant temperature ( $25^\circ\text{C}$ ). The measurement was performed with a steady increment of shear rate ( $\dot{\gamma}$ ); to which, the rate was increased in every  $1 \text{ s}^{-1}$  over the shear-rate range of  $1$ – $10 \text{ s}^{-1}$ , every  $10 \text{ s}^{-1}$  over  $10$ – $100 \text{ s}^{-1}$  and every  $100 \text{ s}^{-1}$  over  $100$ – $1000 \text{ s}^{-1}$ . The rheological properties were all measured after 20 s of duration when shear rate reached each pre-determined rate level over the entire shear-rate range investigated.

## 3. Results and discussion

The  $\text{TiO}_2$  nanoparticle–silica sol mixtures generally exhibited a shear-thinning flow behavior over the shear-rate

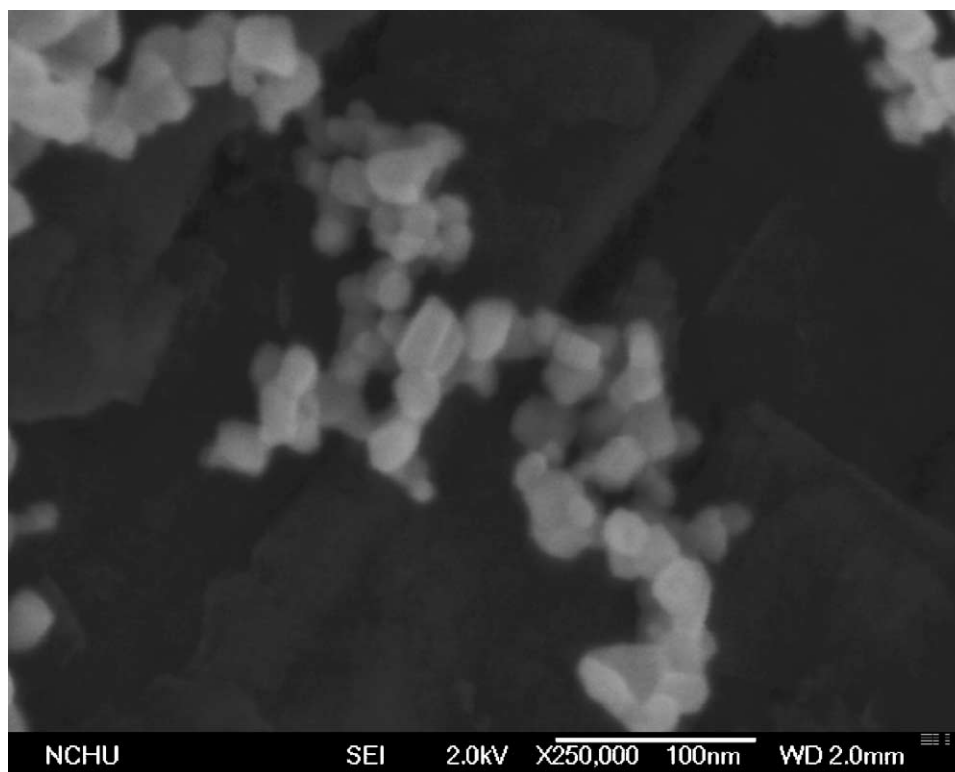


Fig. 1. Particle morphology of the  $\text{TiO}_2$  nanoparticles used in the study.

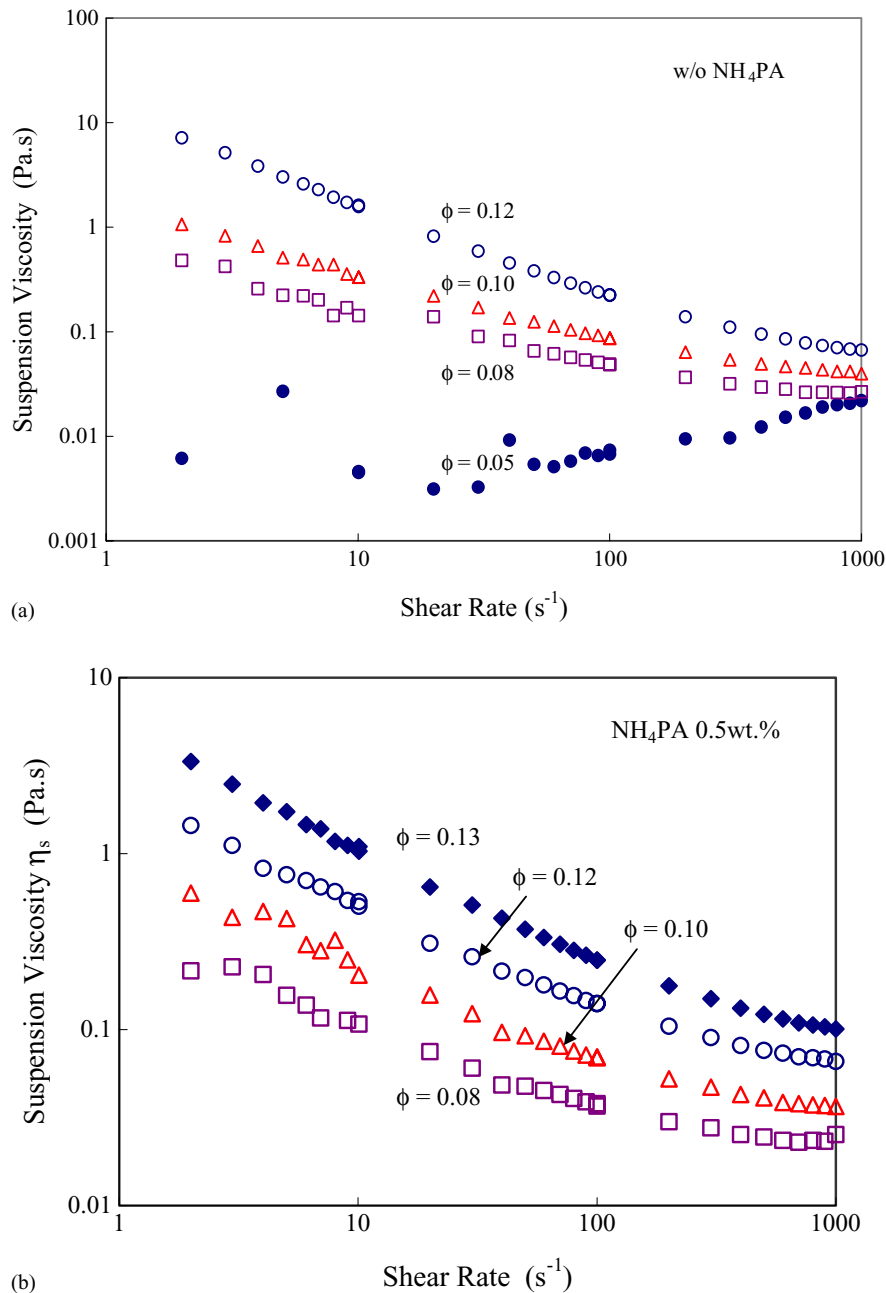


Fig. 2. The  $\eta_s$ – $\dot{\gamma}$  dependence for the particulate sol mixtures of various solids concentrations. (a) Without the NH<sub>4</sub>PA; (b) with 0.5 wt.% NH<sub>4</sub>PA.

range examined (Fig. 2). This indicates that the powder agglomerates existing in the sol liquid were broken up into smaller flow units by the increased shear force, hence resulted in the reduction of suspension viscosity ( $\eta_s$ ) as shear rate increased. In Fig. 2, the addition of NH<sub>4</sub>PA appeared not to alter the shear-thinning flow character of the suspensions; nonetheless,  $\eta_s$  apparently reduced upon the NH<sub>4</sub>PA addition when comparing the viscosity of the suspensions at identical solids loadings. In addition, the introduction of anatase TiO<sub>2</sub> nanoparticles to the silica sols appeared not to catalyze the sols transforming into a gelled network structure. This was most apparent when the suspensions were

highly concentrated. Taking the NH<sub>4</sub>PA-doped suspensions with  $\phi = 0.13$  as an example (Fig. 2b), the suspensions initially showed a solid-like characteristic when the nanoparticles were first introduced into the sol–NH<sub>4</sub>PA liquid mixtures. The nanoparticle suspensions then became apparently “flowable”, i.e., resembled the flow of a concentrated paste, when subjected to the ball-mixing process. The lack of catalyzing effect further reveals that the dominant factor determining the suspension rheology was most likely the interparticle attractions involved in the powdered mixtures. This is considered valid when a low level of NH<sub>4</sub>PA doping ( $\leq 0.5$  wt.%) existed in the nanoparticle-sol suspensions.

It may be interesting to note that the suspensions appeared to change toward a Bingham-plastic (or even a shear thickening) flow from the shear-thinning flow behavior as shear rate further increased toward the higher end. This suggests that the particle-packing configuration in the sol liquid tended to become more uniform in the packing efficiency as shear rate increased. As the particulate structure becomes more uniform, the suspension flow would become less sensitive to the applied shear rate, hence approaching toward a Bingham-like flow. Additionally, the shear thickening flow was likely due to a perturbation occurring in the uniformly packed suspension structure as shear rate exceeded a critical level [9]. A more voluminous flow was resulted, leading to an increase in the flow resistance and accordingly a viscosity increase. Noted that the viscosity scattering found at the low shear rates for the less concentrated  $\phi = 0.05$  suspension (Fig. 2a) was mainly because of the viscosity measured fell in a range of the lower bound of the detecting sensor employed, and was considered only good for reference purposes.

The nanoparticle suspensions began to flow as the applied stress exceeded a certain critical level, i.e., the yield stress ( $\tau_y$ ) of the suspensions. Various empirical models were used to estimate  $\tau_y$  [10]:

Bingham plastic model:

$$\tau = \tau_{y,b} + \eta_s \dot{\gamma} \quad (1)$$

Casson model:

$$\tau^{1/2} = \tau_{y,c}^{1/2} + (\eta_s \dot{\gamma})^{1/2} \quad (2)$$

Herschel-Bulkley model:

$$\tau = \tau_{y,h} + K \dot{\gamma}^n \quad (3)$$

where  $\tau_{y,b}$ ,  $\tau_{y,c}$  and  $\tau_{y,h}$  are yield stress parameters determined from Bingham, Casson and Herschel-Bulkley models, respectively;  $K$  and  $n$  are structure-dependent parameters that can be determined experimentally. As shown in Table 1,  $\tau_y$  increases with  $\phi$ , regardless of the models used. This increase becomes much pronounced as  $\phi$  increased above 0.10, indicating that the suspension  $\tau_y$  is critically dependent on  $\phi$ . The  $\text{NH}_4\text{PA}$  addition appears to result in a  $\tau_y$  reduction.

Table 1

The yield stress of the nanoparticle–sol mixtures determined from various models

Solids concentration ( $\phi$ )	Suspension yield stress $\tau_y$ (Pa)		
	Bingham model	Casson model	Herschel-Bulkley model
0.05	0 (N.A.)	0.01 (N.A.)	0 (N.A.)
0.08	1.7 (1.0)	0.7 (0.3)	1.6 (1.0)
0.10	3.6 (2.4)	1.8 (1.1)	3.1 (2.1)
0.12	15.9 (5.4)	12.1 (2.5)	15.4 (4.6)
0.13	N.A. (11.4)	N.A. (6.1)	N.A. (9.9)

The numbers in parentheses are yield stresses of mixtures with 0.5 wt.%  $\text{NH}_4\text{PA}$ . N.A.: not applicable.

Since  $\tau_y$  is considered the stress required for the nanoparticles to break up the interparticle bonds in order for the particles to roll over the neighboring ones in given carrier liquid under shear forces, a decreased  $\tau_y$  value is thus an indication of a more relaxed particulate structure in the flocculated suspensions. Noted that the Bingham plastic model appears to present the highest yield stress among all the above models examined (Table 1), presumably due to the assumed linear  $\tau$ – $\dot{\gamma}$  dependence in the equation used as  $\tau > \tau_y$ .

Relative viscosity of the suspensions ( $\eta_r$ ) can be defined as the suspension viscosity ( $\eta_s$ ) divided by the viscosity of the suspending liquid ( $\eta_o$ ). As shown in Fig. 3,  $\eta_r$  of the nanoparticle–sol mixtures exhibited a non-linear dependence with  $\phi$ , and (again) the non-linearity appeared to become more pronounced as  $\phi > \sim 0.1$ . A model proposed recently by Liu [11] was used in the study to predict the theoretical, maximum solids fraction ( $\phi_m$ ) allowable for the powdered suspensions. The equation has a general form:

$$\eta_r = [a(\phi_m - \phi)]^{-m} \quad (4)$$

where  $a$  is a constant, and  $m$  is a flow-dependent parameter. The term  $(\phi_m - \phi)$  is physically reasoned as the effective space allowable for the particles to move freely in given carrier medium for the flow to occur. When  $\phi$  approaches  $\phi_m$ ,  $\eta_r$  approaches infinity. The suspension hence ceases to flow and behaves solid-like.  $\phi_m$  can be determined from a  $(1 - \eta_r^{-1/m})$ – $\phi$  relationship, which often follows a linear relationship over a broad range of particle fractions [12,13]. Fig. 4 shows the experimentally determined  $(1 - \eta_r^{-1/m})$ – $\phi$  dependence by assuming the flow index ( $m$ ) equals to 2. The flow index generally falls in a range of  $m = 2$ –3 [11–13]. By extrapolating the  $1 - \eta_r^{-1/2}$  to unity,  $\phi_m$  is determined as  $\phi_m = 0.127$ – $0.162$  at  $\dot{\gamma}$  of  $100 \text{ s}^{-1}$ . The  $\phi_m$  determined is critically dependent on the  $\text{NH}_4\text{PA}$  concentration, and the incorporation of  $\text{NH}_4\text{PA}$  in the sol liquid appears to result in an increase of  $\phi_m$ .

$\eta_s$  of the nanoparticle–sol mixtures alters upon a further increase of  $\text{NH}_4\text{PA}$  concentration above 0.5 wt.% (Fig. 5). A pronounced viscosity decrease occurred when the  $\text{NH}_4\text{PA}$  concentration exceeded 1.0 wt.% and reached a minimum ( $\sim 85\%$  viscosity reduction at  $\dot{\gamma}$  of  $10 \text{ s}^{-1}$ ) as the concentration was of 2.5 wt.%. Noted that the viscosity reduction was still a “respectable” 62% when the shear rate was increased to  $100 \text{ s}^{-1}$ , even though the viscosity change in absolute values appeared less pronounced than that of the  $\dot{\gamma} = 10 \text{ s}^{-1}$  case. The suspension viscosity yet rapidly increased to about the same level as that of the suspensions without the  $\text{NH}_4\text{PA}$  doping as the  $\text{NH}_4\text{PA}$  concentration approached 3 wt.%. Further increase of the  $\text{NH}_4\text{PA}$  concentration to the nanoparticle–sol mixtures only resulted in an immediate formation of a solid-like “bulk”, which virtually showed no evidence of fluid-like deformation upon an excessive shearing. Exact mechanisms about the sol-to-gel transition are not clear at present; nonetheless, two types of gelation schemes are generally considered responsible for the sol–gel derived

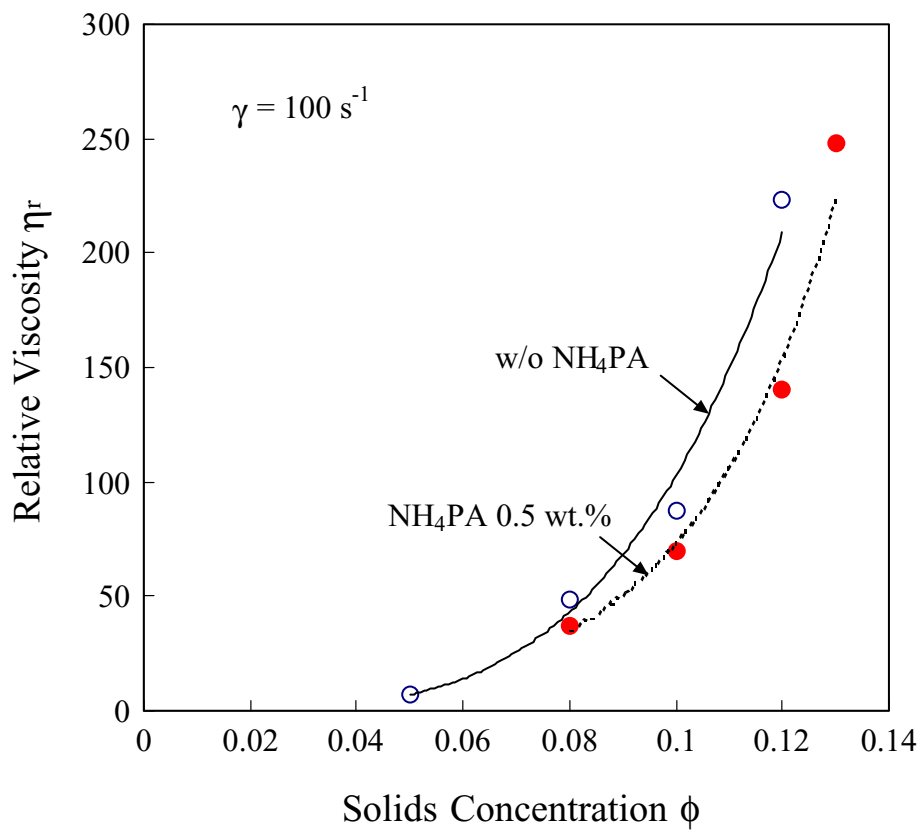


Fig. 3. The  $\eta_r$ – $\phi$  dependence of the particulate sol mixtures at  $\dot{\gamma}$  of  $10 \text{ s}^{-1}$ .

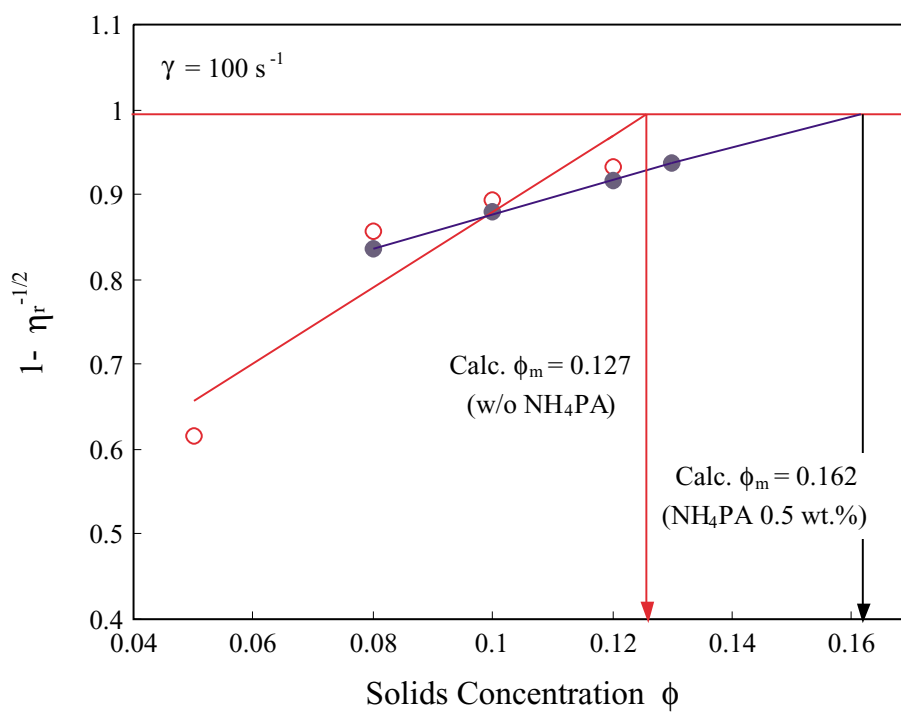


Fig. 4. The  $(1 - \eta_r^{-1/2})$ – $\phi$  dependence for the determination of the maximum solids concentration ( $\phi_m$ ).

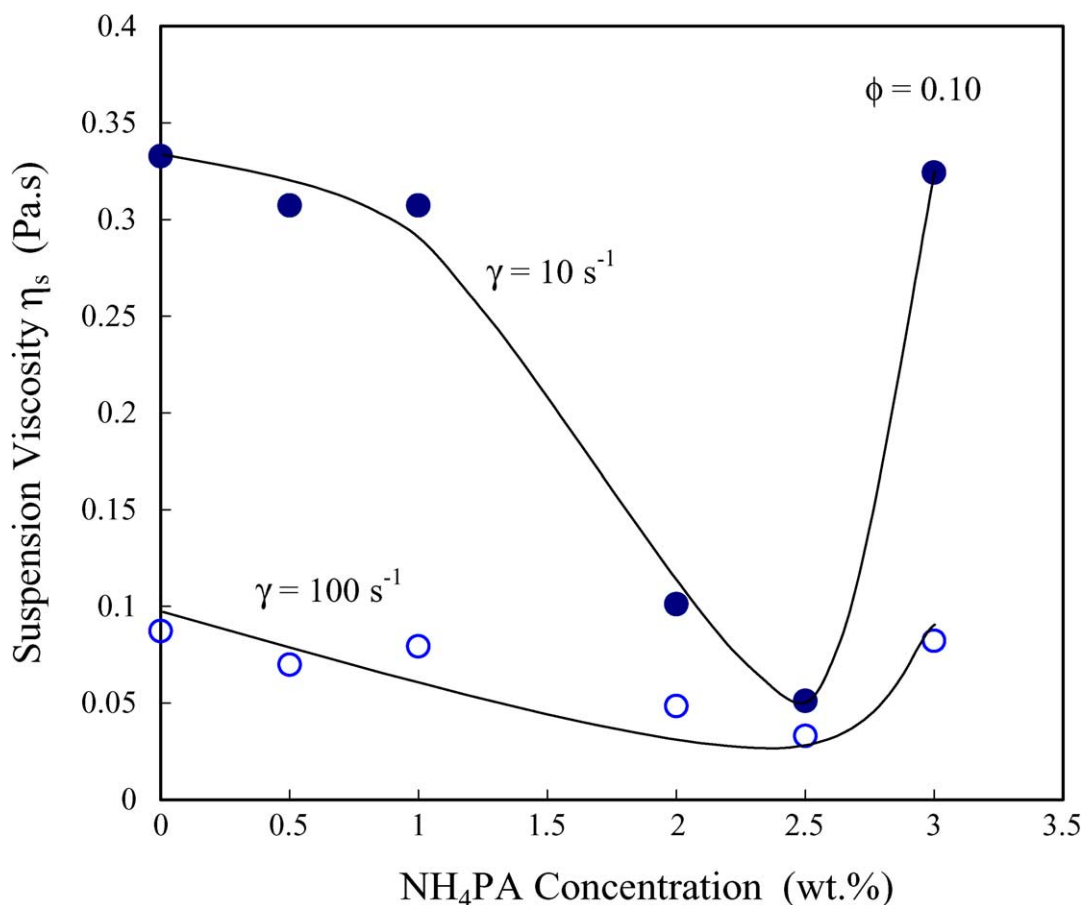


Fig. 5. The  $\eta_s$  of the particulate sols varies with the  $\text{NH}_4\text{PA}$  concentration at shear rates of 10 and  $100 \text{ s}^{-1}$ .

glasses [14]: (1) hydrolysis and polymerization of silicon alkoxides to form a covalent-bonded crosslinked gel; (2) aggregation of particulate sols existing in an aqueous medium to form a porous aggregate structure composed of an interconnected three-dimensional network of hydrogen-bonded crosslinks. A separate experiment by mixing the sol liquid solely with the  $\text{NH}_4\text{PA}$  revealed that the sol quickly changed to gel as the  $\text{NH}_4\text{PA}$  concentration  $> 3.0 \text{ wt.}\%$ . This finding reveals that the  $\text{NH}_4\text{PA}$  served as an effective surfactant to the  $\text{TiO}_2$  nanoparticle–silica sol mixtures only when the concentration was held below a certain extent (i.e.,  $\leq 2.5 \text{ wt.}\%$  in our model mixtures). Further increase of the  $\text{NH}_4\text{PA}$  above the critical level facilitated catalysis of the sol liquids by possibly the hydrolysis and polymerization of the silicon sols into a gelled crosslink structure, so the nanoparticle–sol mixtures turned into a solid-like bulk character.

#### 4. Conclusions

The rheological behavior of anatase-structured  $\text{TiO}_2$  nanoparticle–silicon sol mixtures was examined when ammonium polyacrylate ( $\text{NH}_4\text{PA}$ ) of various concentrations was introduced into the particulate sols. The  $\text{NH}_4\text{PA}$  appeared to facilitate the suspension flow by reducing the

$\text{TiO}_2$  agglomerates into smaller floc units, so that the flow resistance was reduced. A theoretical maximum solids concentration was accordingly resulted ( $\phi_m$  increased from 0.127 to 0.162) when  $\text{NH}_4\text{PA}$  of 0.5 wt.% was added into the particulate sol mixtures. The viscosity reduction was most pronounced when the  $\text{NH}_4\text{PA}$  concentration was held under 2.5 wt.% of the solids at  $\phi = 0.1$ . A rapid sol–gel transition was found when the  $\text{NH}_4\text{PA}$  concentration exceeded the critical level ( $\geq 3.0 \text{ wt.}\%$ ), and the transition was most likely due to the hydrolysis and polymerization of the silicon sols.

#### Acknowledgements

The authors gratefully acknowledge financial support from the National Science Council (Taiwan) under contract NSC 91-2216-E-005-023.

#### References

- [1] C. Anderson, A.J. Bard, An improved photocatalyst of  $\text{TiO}_2/\text{SiO}_2$  prepared by a sol–gel synthesis, *J. Phys. Chem.* 99 (1995) 9882–9885.

- [2] X. Fu, L.A. Clark, Q. Yang, M.A. Anderson, Enhanced photocatalytic performance of titania-based binary metal oxides:  $\text{TiO}_2/\text{SiO}_2$  and  $\text{TiO}_2/\text{ZrO}_2$ , *Environ. Sci. Technol.* 30 (1996) 647–653.
- [3] A.J. Frank, I. Willner, Z. Goren, Y. Degani, Improved charge separation and photosensitized  $\text{H}_2$  evolution from water with  $\text{TiO}_2$  particles on colloidal  $\text{SiO}_2$  carriers, *J. Am. Chem. Soc.* 109 (1987) 3568–3573.
- [4] C. Minero, F. Catozzo, E. Pelizzetti, Role of adsorption in photocatalyzed reactions of organic molecules in aqueous  $\text{TiO}_2$  suspensions, *Langmuir* 8 (1992) 481–486.
- [5] E. Matijević, Q. Zhong, R.E. Partch, Preparation of uniform colloidal dispersions by chemical reactions in aerosols. VI. Silica/titania composite particles, *Aerosol Sci. Technol.* 22 (1995) 162–171.
- [6] R. Mariscal, M. López-Granados, J.L.G. Fierro, J.L. Sotelo, C. Martos, R. Van Grieken, Morphology and surface properties of titania–silica hydrophobic xerogels, *Langmuir* 16 (2000) 9460–9467.
- [7] W.R. Richmond, R.L. Jones, P.D. Fawell, The relationship between particle aggregation and rheology in mixed silica–titania suspensions, *Chem. Eng. J.* 71 (1998) 67–75.
- [8] D. Hotza, P. Greil, Aqueous tape casting of ceramic powders, *Mater. Sci. Eng. A* 202 (1995) 206–217.
- [9] R.L. Hoffman, Discontinuous and dilatant viscosity behavior in concentrated suspensions. 1. Observation of a flow instability, *Trans. Soc. Rheol.* 16 (1972) 155–173.
- [10] J.S. Reed, *Principles of Ceramics Processing*, Wiley, New York, USA, 1995.
- [11] D.-M. Liu, Particle packing and rheological property of highly-concentrated ceramic suspensions:  $\phi_m$  determination and viscosity prediction, *J. Mater. Sci.* 35 (2000) 5503–5507.
- [12] W.J. Tseng, S.-Y. Li, Rheology of colloidal  $\text{BaTiO}_3$  suspension with ammonium polyacrylate as a dispersant, *Mater. Sci. Eng. A* 333 (2002) 314–319.
- [13] W.J. Tseng, C.-N. Chen, Rheology and suspension structure of nickel–terpineol mixtures, *Mater. Sci. Eng. A* 347 (2003) 145–153.
- [14] S.A. Khan, R.K. Prud'Homme, E.M. Rabinovich, M.J. Sammon, Rheology of the gelation of fluorine-doped silica sols, *J. Non-Cryst. Solids* 110 (1989) 153–162.